Energetics of the Nanocrystalline Titanium Dioxide/Aqueous Solution Interface: Approximate Conduction Band Edge Variations between $H_0 = -10$ and $H_- = +26$

L. Andrew Lyon and Joseph T. Hupp*

Department of Chemistry, Northwestern University, Evanston, Illinois 60208

Received: March 9, 1999

A reflectance method has been used to assess conduction band edge energies (E_{cb}) for nanocrystalline TiO_2(anatase) electrodes in contact with aqueous electrolytes. The measurements, which were made over a range of nearly 40 pH units, reveal a Nernstian dependence of E_{cb} upon pH over most of this range, i.e., a −64 mV shift per unit decrease in log(proton activity) between $H_0 = -8$ and $H_- = +23$. Electrochemical quartz crystal microbalance (EQCM) measurements have established that charge compensating proton uptake occurs at potentials negative of E_{cb}. Uptake occurs over the entire EQCM-accessible pH range ($H_0 = -5$ to pH = +11). The combined findings are inconsistent with E_{cb} control solely via surface protonation and deprotonation reactions, whose pK_a's occur in the vicinity of pH 4 and 10. They are consistent, however, with a mechanism whereby: (a) electrochemical generation of Ti(III) trap sites, in the log(proton activity) range from $H_0 = -8$ to $H_- = +23$, is accompanied quantitatively by proton intercalation, (b) conversion of the trap sites back to oxidation state IV is accompanied quantitatively by proton expulsion, and (c) the conduction band edge energy is controlled by the pH-dependent trap-based Ti(III/IV) couple. The pH independence found for E_{cb} above $H_- = +23$ and below $H_0 = -8$ is ascribed to an eventual decoupling of proton intercalation from electron addition.

Introduction

The electronic energetics of metal-oxide semiconductor electrode/aqueous solution interfaces, e.g., absolute valence band and conduction band edge locations, are known to vary systematically with solution pH. The energy dependence is often described as "Nernstian", meaning that band edges shift negatively by about 60 mV per unit increase in solution pH when potentials are evaluated against a pH-independent reference. Interestingly, the Nernstian behavior appears to be a universal characteristic of metal-oxide semiconductor/aqueous solution interfaces. It has been observed for single-crystal electrodes, polycrystalline electrodes, and high surface area nanocrystalline semiconductor electrodes and has been reported for electrodes composed of TiO_2, $SrTiO_3$, SnO_2, WO_3, and ZnO.[1] Explanations for the Nernstian effect have tended to focus on the chemistry of terminal oxo and hydroxo groups,[2] especially their abilty to alter surface charge by adsorbing or desorbing protons (eqs 1 and 2).

$$TiO_2\ (\text{surface}) + H^+ \rightleftarrows TiO(OH)\ (\text{surface}) \quad (1)$$

$$TiO(OH)\ (\text{surface}) + H^+ \rightleftarrows TiO(OH_2)\ (\text{surface}) \quad (2)$$

Here we report on the dependence of the conduction band edge energy of nanocrystalline titanium dioxide (anatase) on pH, H_0, or H_- over an exceptionally wide range of solution acidity and basicity, nearly 40 pH units. This particular material has attracted considerable attention in the context of dye-sensitized photoelectrochemical energy conversion[3] and in the context of fundamental interfacial electron transfer studies.[4,5] In any case, we find for nanocrystalline TiO_2 that Nernstian-type behavior persists over an extraordinarily wide range of pH, well beyond those where open-circuit surface protonation or deprotonation (eqs 1 and 2) would be expected to alter interfacial charges significantly. We also find, via electrochemical quartz crystal microbalance (EQCM) measurements, that addition of electrons to the material stimulates the reversible uptake of protons at near band edge trap sites,[6] even under conditions where *surface* adsorption of protons is not plausible. We propose that the electrochemically stimulated uptake phenomenon represents the dominant mechanism for pH-induced band edge energy variations for the nanocrystalline system.

Experimental Section

Electrolyte Solutions. To achieve both high and low proton activities, standard tables of the Hammett acidity parameters H_0 and H_ were used.[7,8] Highly acidic solutions ($H_0 = -1$ to −10) were prepared by adjusting the concentration of aqueous sulfuric acid solution.[8] Care was taken to cool these solutions during preparation as the mixing of sulfuric acid and water is highly exothermic. To avoid ion pairing effects no additional electrolyte was added. Solutions with very low proton activity (H_ = 15 to 27) were prepared from mixtures of dimethyl sulfoxide (dmso) and water with a fixed total tetramethylammonium hydroxide concentration of 0.11 M.[8] H_ was controlled by changing the ratio of dmso to water. These mixtures were prepared in Teflon labware to avoid leaching of ions from borosilicate glass or Pyrex. (Solutions stored in containers other than Teflon turned yellow.) Electrolyte solutions used in the normal pH range were as follows: pH = 1−2: $HClO_4$, H_2SO_4, or HCl pH-adjusted with NaOH; pH = 13−14: NaOH pH-adjusted with HCl; pH = 3−4: citric acid/NaOH; pH = 4−6: sodium acetate/acetic acid; pH = 6−9: Na_2HPO_4/NaH_2PO_4; and pH = 9−12: $Na_2CO_3/NaHCO_3$. All buffer components were purchased from Aldrich or Fisher and used as received.

TiO_2 Electrodes. Measurements of E_{cb} were performed on three types of nanocrystalline electrodes. The first were prepared

10.1021/jp9908404 CCC: $18.00
Published on Web 05/07/1999

by depositing (spin-coating) colloidal TiO_2 onto a gold-coated electrode platform. The required colloidal suspensions were prepared via a literature method[9] which yielded ~25 g of dialyzed TiO_2 per liter of solution. These samples were then further concentrated to 50−75 g/L. Triton X-100 (surfactant) was then added (1 drop per mL). The platform was composed of quartz with 50 angstroms of Cr vapor deposited as a keyhole shaped adhesion layer over which 1000 angstroms of Au was vapor deposited. All $Au/Cr/SiO_2$ samples (QCM crystals) were purchased from International Crystal Manufacturing. After samples were coated with TiO_2, they were baked in air at 450 °C for 2−4 h. These samples have the advantage of a highly reflective underlayer which facilitates E_{cb} assessment via near infrared reflectance spectroelectrochemistry. However, the films were often not stable enough for prolonged exposure to highly acidic media. In basic media the quartz platform was unstable with respect to dissolution. Consequently, these electrodes were used only between $H_0 = -5$ and pH = +11.

A second set was prepared in the same fashion, except that indium-doped tin oxide (ITO) on glass was used as the electrode platform. As with the TiO_2/Au electrodes, these electrodes could not be used in highly basic media. They were, however, surprisingly stable in acidic media. The excellent signal-to-noise ratio offered by these transparent electrodes allowed confirmation of results obtained with TiO_2/Ti electrodes in acidic media.

A third set of electrodes was prepared by first dissolving 2.3 mL $TiCl_4$ in 10 mL ethanol and then diluting to 50 mg/mL. Titanium rods (6.4 mm diameter) that had been cleaned by soaking for 30 min in boiling 18% HCl were then dipped in the Ti(IV)-containing solution. The coated surfaces were exposed to a 50% humidity atmosphere for 30 min and then heated in air to 450 °C for 20 min. The coating, drying, and heating protocol was repeated nine times, with heating extended to 30 min following the tenth coating. The electrodes were further heated (35 min) in an Ar atmosphere at 550 °C, cooled, and then encased in Kel-F (a fluoropolymer resin) and Torr-Seal (a low volatility epoxy distributed by Varian). Back electrode contact was made with a wire attached with silver epoxy. Raman measurements established that the coatings were anatase. The chief virtue of these electrodes is that they are extremely robust, resisting attack even by the exceptionally caustic solutions used here. Unfortunately, the electrodes are black and, therefore, not very reflective. Consequently, reflectance signals from these electrodes were smaller than those obtained from electrodes prepared on gold platforms.

Potential Measurements. Potentials were controlled with a PAR 273 potentiostat connected to a conventional one-compartment, three-electrode cell. Problems with glass cell instability at the highest pH (H_-) values were avoided by utilizing a cell-less inverted drop configuration: A bead of electrolyte solution was placed on an open working electrode platform, and sharpened reference and counter electrode tips were inserted directly into the bead. E_{cb} was evaluated by scanning the working electrode at 5 to 10 mV/s and recording the reflectance signal generated by 786 nm diode laser illumination. Addition of near infrared absorbing electrons to the conduction band or trap sites leads to an attenuation of reflected light intensity. As described previously,[10a] the potential for the onset of reflectance attenuation was equated with E_{cb}. These measurements were augmented with current vs potential measurements and with electrochemical quartz crystal microbalance (EQCM) measurements. The EQCM experiment reports on electrochemically induced changes in working electrode mass.[11] The EQCM apparatus used here has been described previously.[10−13]

Intercomparison of electrochemical potentials obtained over widely varying ranges of proton activity and ionic strength is inherently problematic because of the difficulty in identifying a universally applicable reference couple. For example, while a conventional saturated (NaCl) calomel electrode (ssce) proved to be adequate as a reference electrode over the $H_0 = -3$ to pH = 11 range, glass instability rendered it unusable at substantially higher pH or H_- values. For extremely acidic solutions (negative H_0 values), on the other hand, we were concerned that varying liquid potentials, associated with variations in solution ionic strength, would introduce significant errors. As a benchmark for the sce response, therefore, we examined the duroquinone/durohydroquinone couple as a function of pH.[7] Because reduction of duroquinone entails the thermodynamically simultaneous addition of two electrons and two protons, the associated formal potential should vary by −59 mV per pH unit versus a pH-independent reference. Furthermore, because both forms of the couple are neutral, the potential should be immune to ion pairing influences and related nonprotic ionic activity effects. In any case, versus the ssce, the duroquinone formal potential shifted by −70 mV per pH unit below $H_0 = -3$. We interpret the modest discrepancy as a probable indication of the existence of a varying liquid junction potential contribution to the ssce-based potentials. Unfortunately, chemical instability precluded the use of the hydroquinone couple below $H_0 = -8$. Ultimately, we found that a silver wire could be employed as a stable pseudo reference electrode provided that the electrode was stored in aq HCl between experiments. In contrast to the ssce, the wire reference yielded a Nernstian response for the duroquinone reduction reaction at extremely negative pH's. Given the surprisingly ideal behavior of the pseudo reference electrode between $H_0 = -8$ and pH = +11, we assumed (admittedly, without direct proof) that the ideal response persisted down to $H_0 = -10$ and up to $H_- = +27$. Notably, the pseudo reference proved to be chemically stable over the entire solution proton activity range. All subsequent measurements at pHs below 1 and above 11, therefore, were made versus the Ag wire reference. Nevertheless, to facilitate comparisons with literature reports, all potentials are reported versus a "corrected" ssce reference, i.e., potentials recorded versus silver were rescaled to reflect a +240 mV difference at pH 7 between potentials measured versus silver and versus ssce. (Thus, the reported potentials have been corrected for the small, liquid junction related error in the ssce reference in solutions more acidic than $H_0 = -3$.)

Results

Approximate Band Edge Energy Measurements. Conduction band edge energy (E_{cb}) assessment via traditional electrochemical impedance methods and related methods is often considered problematic for high porosity, nanocrystalline semiconducting materials.[14] The problems stem, in part, from the nonidealities introduced in impedance responses by high surface area electrode configurations. They also stem from the inability to establish appreciable potential drops across the space charge layers of moderately doped, nanometer scale electrode particles;[15] recall that traditional impedance approaches, such as Mott−Schottky methods, rely upon externally tunable space charge layer effects to generate measurable potential-dependent capacitive responses and that the required space charge layers typically extend for microns in electrodes composed of semiconductor materials of macroscopic dimensions. Recently, however, Fitzmaurice and co-workers have shown that E_{cb} values for nanocrystalline titanium dioxide electrodes can be

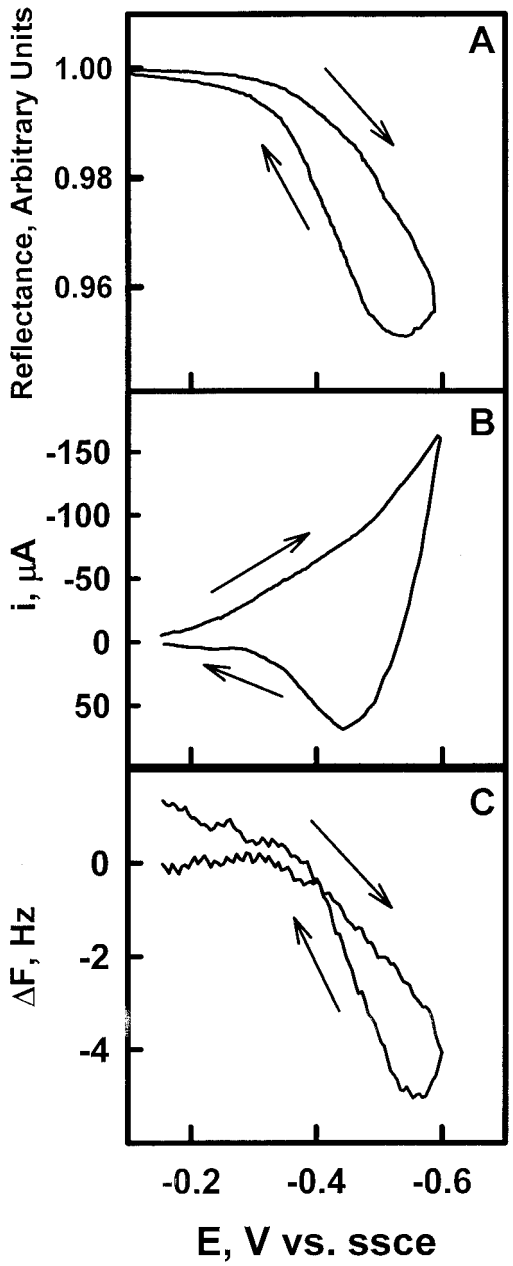

Figure 1. (A) Potential depenedent reflectance (786 nm) of a nanocrystalline TiO_2 film in 0.1 M $HClO_4$. Scan rate = 50 mV/sec. (B) Cyclic voltammogram recorded simultaneously with the reflectance scan in panel A. (C) Potential dependent frequency response of a TiO_2-coated crystal, recorded simultaneously with the data in panels A and B.

estimated by optically monitoring the appearance of electrons associated with near band edge trap sites.[16] Indeed, excellent agreement has been reported between the conduction band edge values obtained optically for nanocrystalline TiO_2 electrodes and those obtained via impedance methods for conventional TiO_2 electrodes.[16] We have adopted the optical approach but have relied upon attenuation of reflected (rather than transmitted) near infrared light to detect trapped electrons.[5d,10a] The reflectance strategy has permitted us to evaluate electrodes prepared on opaque platforms.

Figure 1A shows the outcome of a representative reflectance versus potential experiment, where the onset potential for reflectance diminution has been identified approximately with E_{cb}. The estimate obtained (−0.35 V) is in good agreement with values reported previously on the basis of absorbance techniques.[16] Figure 1B shows the corresponding voltammetric response, which appears to be a combination of so-called capacitive current (reversible) and faradaic current (irreversible hydrogen evolution). Figure 2 illustrates the dependence of E_{cb} on solution acidity (basicity) as measured by pH, H_0, and H_-. Remarkably, the potential varies systematically with log(proton activity) from ca. $H_0 = -8$ to $H_- = +23$. Furthermore, the slope is nearly Nernstian (-64 ± 2 mV per pH (H_0; H_-) unit). Above $H_- = +23$ and below $H_0 = -8$, on the other hand, the potential of the conduction band edge appears to be pH invariant.

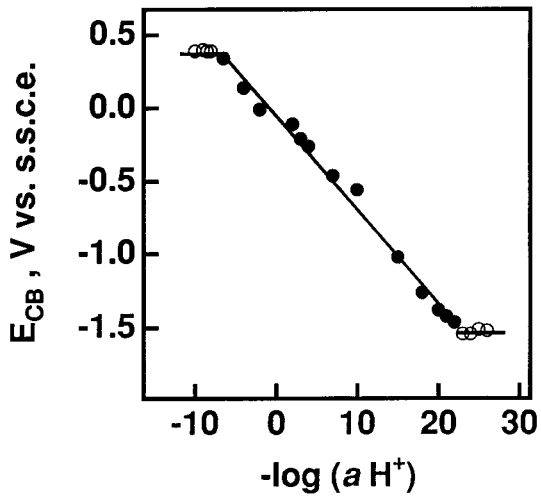

Figure 2. Dependence of reflectance-derived conduction band edge energy on log(proton activity).

EQCM Measurements. Figure 1C illustrates an EQCM experiment run simultaneously with the reflectance and voltammetry experiments shown in panels A and B of the same figure. Notably, a reversible oscillator frequency decrease, corresponding to a mass increase, occurs at approximately the same potential as both the capacitive current onset and the onset of reflectance attenuation. The onset potential for the frequency decrease can be regarded, therefore, as a rough measure of E_{cb}.

Observation of a mass increase implies that adsorption or intercalation of a solution phase species accompanies the addition of electrons to the nanocrystalline electrode material. We note that electrochemical intercalation of alkali metal cations from nonhydroxylic solvents[10] and photochemical uptake of protons from water[12] have previously been demonstrated, via QCM measurements, for nanocrystalline anatase. In principle, the chemical identity, or at least the mass, of the species intercalated or adsorbed here can be determined from the slope of a plot of the change in oscillator frequency versus the amount of charge passed. The assumptions inherent to this approach are (a) that uptake is electrostatically stoichiometric, i.e., each added electronic charge is exactly compensated by an ionic charge and (b) that the Sauerbrey equation,[17] which assumes uniform mass loading on a flat surface, is quantitatively applicable. The second assumption, in particular, seems unlikely to be fully met. Nevertheless, assuming that the species taken up is monocationic, the mass obtained from multiple Saurbrey analyses ranges from 1 to 3 g/mol. A mass of 1 g/mol obviously suggests uptake of protons. To test the idea, additional comparative experiments were run with unbuffered D_2O vs H_2O as solvent and $LiClO_4$ as electrolyte (Figure 3). The approximately 2 to 1 ratio establishes that the electrointercalated or adsorbed species indeed is $D^+(H^+)$.

In Figure 4, the QCM-derived onset potential for reversible ionic uptake has been used to estimate E_{cb} as a function of pH.[10,12] The measurements were made in the presence of either

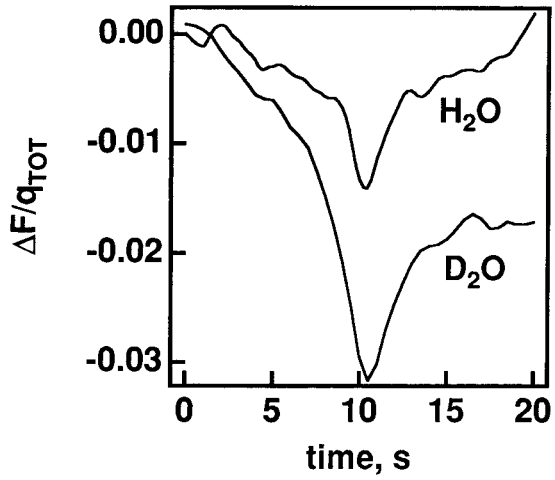

Figure 3. Comparison of charge (q_{TOT}) normalized QCM frequency shifts during reversible potential scanning of a TiO_2-coated crystal in contact with H_2O or D_2O. Electrolyte is 0.1 M $LiClO_4$.

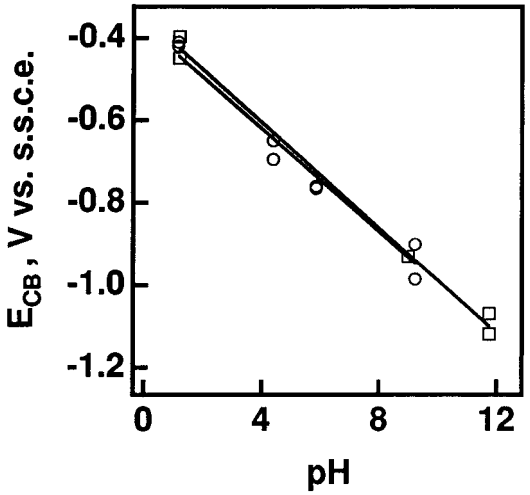

Figure 4. Dependence of EQCM-derived conduction band edge energy on pH. Background electrolyte: (□) 1.0 M $NaClO_4$; (○) 2.0 M $LiClO_4$.

1.0 M $NaClO_4$ or 2.0 M $LiClO_4$ (plus the appropriate acid, base, or buffer).[18] The summary results in Figure 4, together with the actual EQCM data, indicate that electrochemically reduced titanium dioxide has an enormous preference for H^+ uptake in comparison to either Li^+ or Na^+ uptake. Indeed, even at pH = 12, where the alkali metal ion activities exceed the proton activity by 12 orders of magnitude, the EQCM experiments indicate that H^+ uptake occurs. Given the vanishingly small free H^+ concentration, the source of protons under these conditions clearly must be the solvent. Unfortunately, attempts to extend the EQCM measurements to even higher pHs were confounded by QCM electrode instability.

EQCM experiments were successfully extended to extremely acidic environments, the most extreme being $H_0 = -6$.[19] Notably, under these conditions: (1) reversible proton uptake was still observed and (2) E_{cb} estimates from EQCM measurements still coincided with E_{cb} estimates from reflectance measurements. Notice that the most extreme measurements were made ~10 pH units below the pK_a for eq 2,[20] i.e., reversible proton uptake was readily observed even under conditions where no *surface* proton accepting sites remained. (While the last observation seems to imply proton insertion or intercalation, we cannot rule out the possibility, especially under less acidic conditions, that the addition of electrons instead induces proton adsorption.)

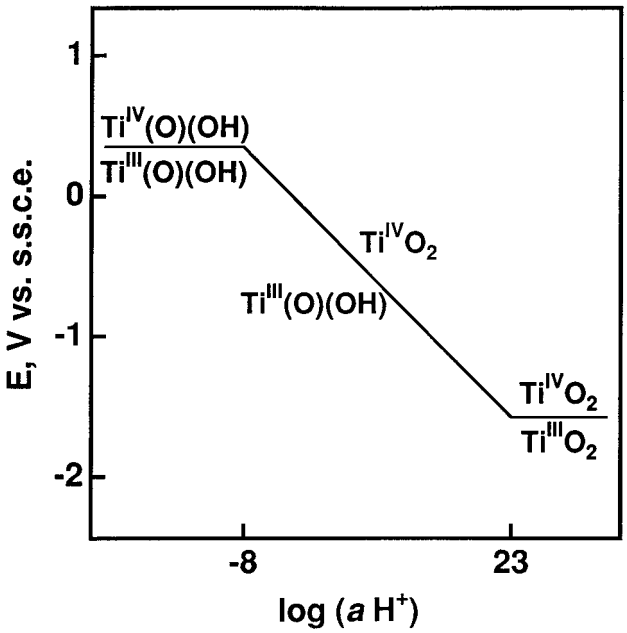

Figure 5. Aqueous redox/protonation phase diagram (Pourbaix diagram) for TiO_2 trap sites engaging in intercalation chemistry.

Discussion

Redox Active Trap States and Band Edge Energetics. The combined spectral, electrochemical, and microgravimetric experiments (Figures 1−4) unequivocally show that electron addition to nanocrystalline titanium dioxide, in contact with a very wide range of aqueous electrolytes, is accompanied by charge compensating proton uptake. If uptake is assumed to involve near band edge trap states (a reasonable assumption in view of the known spectral characteristics (ESR, absorption, and attenuance) of "reduced" nanocrystalline films[14,16]), then the coupled uptake process can be written in the molecular limit as the following:

$$Ti^{IV}O_2 + e^- + H^+ \rightleftarrows Ti^{III}(O)(OH) \quad (3)$$

This leads to the interesting prediction that the potential associated with trap filling will vary with pH; consistent with experiment (Figures 2 and 4), the expected shift is −59 mV per pH unit.

The pH dependence should persist until either the Ti^{IV} form of the trap site is protonated (eq 4) or the Ti^{III} form is deprotonated (eq 5). The corresponding electron uptake reactions are then eqs 5 and 6.[21] Equations 3−7 are summarized in Figure 5 in the form of a redox/protonation "phase" diagram

$$Ti^{IV}O_2 + H^+ \rightleftarrows Ti^{IV}(O)(OH) \quad (4)$$

$$Ti^{III}(O)(OH) \rightleftarrows Ti^{III}O_2 + H^+ \quad (5)$$

$$Ti^{IV}(O)(OH) + e^- \rightleftarrows Ti^{III}(O)(OH) \quad (6)$$

$$Ti^{IV}O_2 + e^- \rightleftarrows Ti^{III}O_2 \quad (7)$$

or Pourbaix diagram. In Pourbaix diagrams, the slopes of the *E* vs pH plots express the proton (p) to electron (n) stoichiometry in the corresponding redox reactions. At 300 K, the slopes are (p/n)59 mV per pH unit. The break points, on the other hand, define the pK_a's of the redox species.

If this interpretation is applied to the anatase data in Figure 2 (and Figures 3 and 4), then between $H_0 = -8$ and $H_- = +23$

the proton coupled electron addition reaction occurs (eq 3). Below $H_0 = -8$, a proton *de*coupled redox reaction occurs (eq 6), while above $H_- = +23$, a slightly different proton decoupled redox reaction occurs (eq 7). Figure 2 further indicates that the pK_a for $Ti^{IV}(O)(OH)$ is ca. -8, while the pK_a for $Ti^{III}(O)(OH)$ is ca. $+23$. Expressed another way, addition of a single electron to $Ti^{IV}O_2$ increases its basicity or proton affinity by more than 30 orders of magnitude (31 pH units). The basicity enhancement, while extremely large, is broadly consistent with the known chemistry of *molecular* metal oxo, hydroxo species. For example, the pK_a of *trans*-$(O)(OH)Re^{VI}(pyridine)_4^{3+}$ increases by an estimated 18 pH units upon addition of one electron and well over 40 pH units upon addition of three electrons.[22,23] In any case, the pK_a jump encountered here implies that $Ti^{III}O_2$ is capable of extracting protons from an enormous range of acids.

The persistence of Nernstian behavior at pH values far above and below the pK_a's of the surface protonation reactions 1 and 2 indicates that the putative band edge controlling reactions (eqs 3−7) differ chemically from eqs 1 and 2. We suggest that reactions 1 and 2 describe proton adsorption processes occurring at the semiconductor/solution interface, but that reactions 3−5 instead involve proton *intercalation*. Support for the intercalation hypothesis exists from analogous studies of Li^+ uptake from nonhydroxylic solvents, including studies indicating that nanocrystalline TiO_2 can be made to function as an intercalation-type battery electrode.[24] If the interpretation is correct, then the enormous differences in pK_a for reaction 2 (adsorption) versus 4 or 5 (intercalation) can be viewed as a measure of the comparative ease (or difficulty) of achieving protonation in an aqueous interfacial environment (eq 1) versus a purely metal-oxide environment (eqs 4 and 5).

We propose that over the pH range -8 to $+23$ the value for E_{cb} for nanocrystalline titanium dioxide is determined primarily by equilibration of the conduction band with the trap-based redox couple shown in eq 3. (A related discussion in ref 14 casts the problem in terms of trap site induced band edge unpinning.) We further speculate that reaction 3 or a similar process controls the band edge energetics at nominally single-crystal titanium dioxide/aqueous solution interfaces. Compelling evidence for space charge layer formation, i.e., charge delocalization, exists for single-crystal rutile electrodes, at least under depletion conditions.[25] This would seem to argue against a redox trap interpretation. Nevertheless, it is conceivable that even a small number of defect or trap sites (localized charge sites) could provide energetic control over the band edge location. Evidence, albeit, not proof, for such control would be the persistence of Nernstian behavior at extreme pHs. To the best of our knowledge, an investigation of single-crystal TiO_2 band edge energetics under extreme pH conditions has not yet been reported.

Proton Adsorption and Band Edge Energetics. While the preceding discussion emphasizes the role of redox-induced proton intercalation in defining band edge energies, significant secondary influences presumably are exerted by the somewhat simpler proton adsorption reactions shown in eqs 1 and 2. The basis for the effect is the net addition of surface charge. (In contrast, the intercalation or insertion process, eq 3, yields no change in overall charge.) Borrowing from the discussion by Kalaysundaram et al., the portion of the oxide surface (ϕ_s^{ox}) − aqueous solution (ϕ^{sol}) potential difference that can be ascribed to adsorbed charge (σ_0) is $\{kT\sigma_0/2\theta N_s e^2\}$ where k is Boltzmann's constant, T is temperature, N_s is the number of ionizable sites per cm^{-2}, θ equals $1/\{(K_{a2}/K_{a1})^{1/2} + 2\}$, K_{a1} and K_{a2} are acid dissociation (proton desorption) constants for TiO(OH) (surface) and $TiO(OH_2)$ (surface), and e is the unit electronic charge.[26,27] The variation with pH is then given by:[26−28]

$$d(\phi_s^{ox} - \phi^{sol})/d\mathrm{pH} = \{kT/2\theta N_s e^2\}(d\sigma_0/d\mathrm{pH}) \qquad (8)$$

Given that reactions 1 and 2 shift to the left as the pH increases, $d\sigma_0/d$pH should be negative and negative shifts in potential should occur with increases in pH. Again from eqs 1 and 2, the shifts should be greatest in the vicinity of the pK_a's for the surface deprotonation reactions. On the other hand, they should become vanishingly small at pHs more than a couple of units removed from the pK_a's, since σ_0 will no longer significantly vary with pH. (The invariance follows from the expectation that at pH $\ll$ pK_{a2} almost all available surface sites will already be protonated, while at pH $\gg$ pK_{a1} almost all available surface sites will be deprotonated.) Thus, eq 8 should yield a pH-dependent potential contribution that resembles the zeta potential and mimics acid/base titration type behavior. The equation does not account, however, for the extended Nernstian behavior observed experimentally. Instead, the equation is most appropriately invoked in the context of discussions of *deviations* from Nernstian E_{cb} behavior.

Conclusions

Reflectance based conduction band edge energy measurements for nanocrystalline TiO_2 show that the energy varies in a Nernstian fashion with log(proton activity) over an enormous solution acidity (basicity) range: ca. 31 pH units. This behavior is inconsistent with E_{cb} control solely via surface protonation and deprotonation reactions. It is consistent, however, with a mechanism whereby: (a) electrochemical generation of Ti(III) trap sites is accompanied quantitatively by H^+ uptake or intercalation, (b) conversion of the trap sites back to oxidation state IV is accompanied quantitatively by proton expulsion, and (c) the conduction band edge energy is controlled by the pH-dependent trap-based Ti(III/IV) couple. The proposed mechanism is supported by EQCM measurements which show that electron addition to near band edge trap sites is indeed accompanied by reversible proton intercalation and by experiments showing that the proton intercalation phenomenon persists at pHs well above the pK_a for surface $Ti^{IV}O(OH)$ species and well below the pK_a for surface $Ti^{IV}O(OH_2)$ species. The pH independence found for E_{cb} above $H_- = +23$ and below $H_0 = -8$ is ascribed to an eventual decoupling of proton intercalation from electron addition.

Acknowledgment. We thank Buford Lemon for help with selected EQCM experiments and for many helpful discussions. We gratefully acknowledge the Office of Naval Research for financial support of our research.

References and Notes

(1) See, for example: (a) Bolts, J. M.; Wrighton, M. S. *J. Phys. Chem.* **1976**, *80*, 2641. (b) Watanabe, T.; Fujishima, A.; Tatsuki, O.; Honda, K. *Bull. Chem. Soc. Jpn.* **1976**, *49*, 8. (c) Gerischer, H. *Electrochim. Acta* **1989**, *34*, 1005. (d) Hardee, K. L.; Bard, A. J. *J. Electrochem. Soc.* **1975**, *122*, 739. (e) Natan, M. J.; Wrighton, M. S. *J. Phys. Chem.* **1987**, *91*, 648.

(2) See, for example: Finklea, H. O. *Semiconductor Electrodes*; Elsevier: New York, 1988; Chapter 2.

(3) For reviews, see: (a) Hagfeldt, A.; Grätzel, M. *Chem. Rev.* **1995**, *95*, 49. (b) Kamat, P. V. *Chem. Rev.* **1993**, *93*, 267. (c) Meyer, G. J.; Searson, P. C. *Interface* **1993**, *2*, 23.

(4) Representative reports: (a) Vinodgopal, K.; Hua, X.; Dahlgren, R. L.; Lappin, A. G.; Patterson, L. K.; Kamat, P. V. *J. Phys. Chem.* **1995**, *99*, 10883. (b) Moser, J.; Grätzel, M. *Chem. Phys.* **1993**, *176*, 493. (c) Argazzi, P.; Bignozzi, C. A.; Heimer, T. A.; Meyer, G. J. *Inorg. Chem.* **1997**, *36*, 2.

(d) Hannappel, T.; Burfeindt, B.; Storck, W.; Willig, F. *J. Phys. Chem., B* **1997**, *101*, 6799.

(5) See also: (a) Blackbourn, R. L.; Johnson, C. S.; Hupp, J. T. *J. Am. Chem. Soc.* **1991**, *113*, 1060. (b) Lu, H.; Preiskorn, J. N.; Hupp, J. T. *J. Am. Chem. Soc.* **1993**, *115*, 4927. (c) Yan, S. G.; Hupp, J. T. *J. Phys. Chem.* **1996**, *100*, 6867. (d) Yan, S. G.; Hupp, J. T. *Proc.-Electrochem. Soc.* **1996**, *96*−*9*, 53.

(6) There is an interesting precedent in the radiation chemistry literature: Borrgello, Pellizzetti, Mulac, and Meisel (*J. Chem. Soc., Faraday Trans. 1* **1985**, *81*, 143) have shown that radiolytic reduction of colloidal TiO_2 induces proton uptake. Photoinduced proton uptake, in this case by a high area, thin film form of titanium dioxide, has also been reported (Lemon, B. I.; Hupp, J. T. *J. Phys. Chem.* **1996**, *100*, 14578).

(7) Laviron, E.; Meunier-Prest, R.; Vallat, A.; Roullier, L.; Lacasse, R. *J. Electroanal. Chem.* **1992**, *341*, 227.

(8) Rochester, C. H. *Acidity Functions*; Academic Press: New York, 1970.

(9) Xu, Q.; Anderson, M. A. *J. Mater. Res.* **1991**, *6*, 1073.

(10) (a) Lyon, L. A.; Hupp, J. T. *J. Phys. Chem.* **1995**, *99*, 15718. (b) Krtil, P.; Kavan, L.; Fattakhov, D. *J. Solid State Electrochem.* **1997**, *1*, 83.

(11) For a review see: Buttry, D. A. In *Electroanalytical Chemistry*; Bard, A. J., Ed.; Marcel Dekker Inc.: New York, 1991; Vol. 17, pp 1−85.

(12) Lemon, B. I.; Hupp, J. T. *J. Phys. Chem. B* **1996**, *100*, 2426.

(13) Ward, M. D. *J. Phys. Chem.* **1988**, *92*, 2049.

(14) See, for example: Cao, F.; Oskam, G.; Searson, P. C.; Stipkala, J. M.; Heimer, T. A.; Farzad, F.; Meyer, T. J. *J. Phys. Chem.* **1995**, *99*, 11974.

(15) (a) Albery, W. J.; Bartlett, P. N. *J. Electrochem. Soc.* **1984**, *131*, 315. (b) Hodes, G.; Howell, I. D.; Peter, L. M. *J. Electrochem. Soc.* **1992**, *139*, 5983.

(16) (a) Enright, B.; Redmond, G.; Fitzmaurice, D. *J. Phys. Chem.* **1994**, *98*, 6195. (b) O'Regan, B.; Grätzel, M.; Fitzmaurice, D. *Chem. Phys. Lett.* **1991**, *183*, 89. (c) Redmond, G.; Fitzmaurice, D. *J. Phys. Chem.* **1993**, *97*, 1426. (d) O'Regan, B.; Grätzel, M.; Fitzmaurice, D. *J. Phys. Chem.* **1991**, *95*, 10525. (e) Rothenberger, G.; Fitzmaurice, D.; Grätzel, M. *J. Phys. Chem.* **1992**, *96*, 5983.

(17) Saurbrey, G. Z. *Z. Phys.* **1959**, *155*, 206.

(18) E_{cb} data obtained in the most highly acidic environments are omitted from Figure 4 because the electrolyte in these environments was composed solely of aq H_2SO_4.

(19) EQCM responses were, in fact, obtained in solutions of more negative H_0 but were complicated by viscous loading effects.

(20) Schindler and Gamsjäger *Faraday Discuss. Chem. Soc.* **1971**, *52*, 286) report for anatase: $pK_{a1} = \{7.8 + 13(-Ti-O^-)\}$ and $pK_{a2} = \{5.0 - 26(-Ti-OH_2^+)\}$, where the concentrations of the fully protonated and fully deprotonated surface species are given in mol/kg. Thus, at any finite concentration of $-Ti-O^-$, the value of pK_{a1} will be greater than 7.8, while at any finite concentration of $-Ti-OH_2^+$, the value of pK_{a2} will be less than 5.0. If one assumes that the acid−base titration data reported by Schindler and Gamsjäger extend to saturation, then the pK_a values for their samples at half saturation (i.e., midpoints of titrations) are 3.9 and 9.7.

(21) A reviewer has pointed out that under neutral and basic conditions eqs 3−5 must be more chemically complicated than indicated, since the needed protons must be abstracted from water molecules (see also, Discussion section). The reviewer has also noted that proton uptake occurs at potentials negative of the reversible potential for the breakdown (reduction) of water to H_2 and has asked us to discuss how the mechanism of water breakdown, and any associated kinetic overpotential, might affect microbalance-based E_{cb} estimates. E_{cb} clearly is a thermodynamic quantity. Its value, therefore, will not depend on the mechanism of proton abstraction, nor will it depend on the source of protons. Instead, only the proton activity should be significant. The approximate experimental reversibility of the interfacial proton uptake/release reaction (Figure 1), as opposed to the kinetic irreversibility of the electrochemical hydrogen evolution reaction, implies that the measured E_{cb} values are equivalent to the desired thermodynamic values.

(22) Ram, M. S.; Skeens-Jones, L. M.; Johnson, C. S.; Zhang, X. L.; Stern, C.; Hupp, J. T. *J. Am. Chem. Soc.* **1995**, *117*, 2171.

(23) See also: Liu, W.; Thorp, H. H. *Inorg. Chem.* **1994**, *33*, 1026.

(24) (a) Huang, S. Y.; Kavan, L.; Exnar, I.; Grätzel, M. *J. Electrochem. Soc.* **1995**, *142*, L142. (b) Macklin, W. J.; Neat, R. J. *Solid State Ionics* **1992**, *53*−*56*, 694.

(25) Lantz, J. M.; Baba, R.; Corn, R. M. *J. Phys. Chem.* **1993**, *97*, 7392.

(26) Kalaysundaram, K.; Grätzel, M.; Pelizetti, E. *Coord. Chem. Rev.* **1986**, *69*, 57.

(27) See also: Healy, T. W.; White, L. R. *Colloid Interface Sci.* **1978**, *9*, 303.

(28) The presentation in ref 26 also includes a term of the form $(\mu^*_{H+})^{ox} - (\mu^*_{H+})^{sol} + (RT/F)\ \ln\{(a_{H+})^{sol}/(a_{H+})^{ox}\}$, where the μ^*'s are standard chemical potentials for the proton on the oxide surface and in solution, F is the Faraday constant, and the a_{H+}'s are proton activities. At 298 K, this term contributes −59 mV per pH unit to E_{cb}, if variations in surface protonation, $(a_{H+})^{ox}$, with pH are neglected. (Note that these variations are already taken into account via eq 8.) In any case, we find that the additional term appears only when electrochemical potentials are evaluated against a reference electrode that is reversible with respect to protons. The term is absent when electrode potentials are evaluated versus a pH-independent reference such as saturated calomel, Ag/AgCl, ferrocene/ferrocenium, silver wire pseudo reference, etc.